Processing and Characterization of Titanium-Hydroxyapatite Metal Matrix Composite for Biomedical Applications

A THESIS SUBMITTED IN PARTIAL FULFILLMENT
OF THE REQUIREMENT FOR THE DEGREE OF

Bachelor of Technology

in

Biotechnology

by

Shammy Raj

109BT0683

Under the Supervision of

Dr. A. Thirugnanam

Department of Biotechnology and Medical Engineering

National Institute of Technology Rourkela

Rourkela, Odisha, 769 008, India

May 2013

Department of Biotechnology and Medical Engineering
National Institute of Technology Rourkela
Rourkela - 769008, Odisha, India.

Certificate

This is to certify that the thesis entitled "**Processing and Characterization of Titanium-Hydroxyapatite Metal Matrix Composite for Biomedical Applications**" by **Shammy Raj (109BT0683),** in partial fulfillment of the requirements for the award of the degree of Bachelor of Technology in Biotechnology during session 2009-2013 in the Department of Biotechnology and Medical Engineering, National Institute of Technology Rourkela, is an authentic work carried out by him under my supervision and guidance. To the best of my knowledge, the matter embodied in the thesis has not been submitted to any other University/Institute for the award of any degree or diploma.

Place: NIT Rourkela
Date: 12th May 2013

Dr. A. Thirugnanam
Assistant Professor
Biotechnology and Medical Engineering
National Institute of Technology
Rourkela-769 008, Odisha (India)

Acknowledgement

Successful completion of this project is the outcome of consistent guidance and assistance from many people, faculty and friends and I am extremely fortunate to have got these all along the completion of the project.

I owe my profound gratitude and respect to my project guide, **Prof. A. Thirugnanam**, Department of Biotechnology and Medical Engineering, NIT Rourkela for his invaluable academic support and professional guidance, regular encouragement and motivation at various stages of this project.

I also thank **Dr. Ashok Kumar Mondal**, Asst. professor, Department of Metallurgical and Materials engineering, NIT Rourkela. I am extremely grateful to him for his consistent guidance and support.

I place on record my sincere gratitude to **Prof. Krishna Pramanik**, Head of Department, Department of Biotechnology and Medical Engineering, NIT Rourkela for her constant encouragement.

I would like to thank Ms. Tejinder Kaur and Mr. Deependra Kumar Ban, Ph.D Scholar Department of Biotechnology and Medical Engineering, NIT Rourkela and Mr. Anil Kumar Singh Bankoti, Ph.D scholar, Department of Metallurgical and Materials engineering, NIT Rourkela for their regular support, help and motivation.

I would also thank my Institution and my faculty members without whom this project would have been a distant reality. I also extend my thanks to my family, friends, and well-wishers.

Finally I would like to express my heartiest thank to my friend Prasanna Chandra Jha for his constant help and encouragement during the project. I thank him for being with me throughout the completion of project.

Place: NIT Rourkela
Date: 12th May 2013

Shammy Raj
109BT0683
Biotechnology and Medical Engineering
National Institute of Technology
Rourkela-769 008, Odisha (India)

Contents

Abbreviations

1.	Ti	–	Titanium
2.	Cp Ti	–	Commercially pure Titanium
3.	Ha	–	Hydroxyapatite
4.	Ti-Ha	–	Titanium Hydroxyapatite
5.	Ti10	–	Titanium Hydroxyapatite with 10 weight% of Hydroxyapatite
6.	Ti15	–	Titanium Hydroxyapatite with 15 weight% of hydroxyapatite
7.	SBF	–	Simulated body fluid
8.	SEM	–	Scanning electron microscopy
9.	XRD	–	X-ray diffraction
10.	Rpm	–	Revolutions per minute
11.	g	–	gram
12.	ml	–	milli liter
13.	mm	–	milli meter
14.	cc	–	centimeter cube
15.	wt.	–	weight
16.	h	–	hours
17.	min	–	minutes

List of Tables

List of Figures

Abstract

Low density, superior mechanical properties, excellent wear and corrosion resistance and low stress shielding of Titanium (Ti) has caused an increase in the use of Ti for biomedical applications. However poor bioactivity of Ti limits its use in load bearing orthopedic implants. Hydroxyapatite (Ha) ($Ca_{10}(PO_4)_6(OH)_2$) possess excellent bioactivity but poor mechanical properties does not allow the use of Ha for load bearing orthopedic implants. In the study, Titanium and Hydroxyapatite (Ti-Ha) composite was prepared using powder metallurgy technique. Three samples of varying Ti and Ha content was ball milled, compacted and sintered. The ball milled and compacted samples were characterized using X-ray diffraction (XRD) and scanning electron microscope (SEM). The density of the composite was measured using Archimedes principle. The *in-vitro* bioactivity studies were assessed in simulated body fluid (SBF) for two weeks. After each week, samples were removed and characterized using SEM for the formation of hydroxyapatite and subsequently phase was confirmed by XRD. The density of the samples decreased with increase in Ha content. However the porosity and bioactivity increased with increase in the Ha content.

Keywords: Titanium, hydroxyapatite, ball milling, simulated body fluid, bioactivity

Chapter 1: Introduction

1.0. Introduction

Aging and accidents are two important causes which lead to injury, damage and disease in the bone tissue. Though bone tissue has a property of regenerative growth and remodeling, it fails in some critical accidents and diseases. One effective approach to solve this problem is grafting. Autografts, allografts and syngrafts are the main approaches to replace lost bones or repairing bone defects. Autografting has good compatibility and it triggers no immunological response; however the limited donor bone supply and the additional trauma involved has limited its application.

Many artificial bone tissues of ceramics and metals are being developed to facilitate bone regenerative growth and bone healing. Biomaterials are natural or synthetic materials engineered to function similar to that of damaged tissue in bio-environment. A material to be used as a biomaterial should have an excellent biocompatibility and bioactivity. Beside these it should also have mechanical properties similar to that of the damaged or diseased bone. High corrosion and wear resistance also plays an important role for biomaterials used in load bearing sites. [1]

Metallic biomaterials are preferred in load bearing orthopedic implants due to good mechanical properties. Metals and alloys that combine high strength with reasonable corrosion resistance are favorite biomaterials for the fabrication of orthopedic implants which are subjected to severe mechanical loading inside the human body. Metallic biomaterials have greatly attracted the researchers and further research is necessary to improve the properties like tensile strength, Youngs' modulus, fatigue fracture, stress shielding, wear and corrosion resistivity, biocompatibility and bioactivity. The materials currently used for surgical implants include calcium phosphate ceramic, 316L stainless steel (316LSS), cobalt chromium (Co–Cr) alloys, magnesium and its alloys and titanium and its alloys [1-2]. Recent advancement in the field of biomaterials has seen the development of titanium-hydroxyapatite (Ti-Ha) composite which possess the blend of excellent mechanical properties of titanium and better bioactivity of hydroxyapatite [3-5].

1.1 Conventional Biomaterials

1.1.1 Stainless steel: The metallic biomaterial most commonly used for orthopedic applications earlier was the austenitic stainless steel. Its utilization is particularly justified by the combination of properties such as good acceptance by the body; low cost; good machinability; good formability; high strength, especially when cold worked and reasonable corrosion resistance. However, some aspects such as low strength in the annealed condition and susceptibility to localized corrosion often limits the wider use of this type of material in orthopedic applications, mainly when the implanted device must remain in the human body for a relatively long time (more than 12 months). The combination of such aspects favors the failure of orthopedic implants by a synergy called as corrosion–fatigue [6]. Ni and Cr are main components of stainless steel. These implants are reported to release these elements due to corrosion in the body. Ni and Cr released from prosthetic implants have been reported to be toxic. Skin related diseases such as dermatitis due to Ni toxicity have also been reported [1]. In addition, 316L SS possess much higher modulus than bone, leading to insufficient stress transfer to bone leading to bone resorption and loosening of implant after some years of implantation. The high cycle fatigue failure of hip implants is also reported as the implants are subjected to cycles of loading and unloading over many years [1].

1.1.2 Cobalt chromium alloys: Co–Cr based alloys are the most commonly used representative of Co alloys for biomedical applications. The presence of Cr imparts the corrosion resistance and the addition of small amounts of other elements such as iron, molybdenum or tungsten can give very good high temperature properties and abrasion resistance. The various types of Co – Cr alloys used for implant applications include Co–Cr–Mo, Co–Cr–Mo, Co–Cr–W–Ni and Co–Ni–Cr–Mo–Ti. Clinical applications of such alloys include its use in dentistry and maxillofacial surgery. However high cost, low formability and poor machinability are some of the limitations, preventing the use of these metallic materials for orthopedic applications. Also like stainless steel, Co and Cr are toxic and causes skin disease. Co has also been reported to be carcinogenic [1].

1.1.3 Magnesium and its alloys: As an important essential trace element, magnesium participates in almost all the human metabolism, ranking just after calcium, sodium and potassium. Its density ($1.74 g/cm^3$) is close to that of natural bone ($1.75 g/cm^3$). Meanwhile, its high specific strength (pure Mg, 133 GPa/ ($g \cdot cm^3$)) and specific stiffness, can meet the strength performance requirements of biological implant materials. As a biodegradable implant material, magnesium provides both biocompatibility and sufficient mechanical properties. Mg alloys are very attractive due to their good biocompatibility and especially their degradability. Researchers found that magnesium alloys offer great potential as absorbable implant materials such as cardiovascular tube stent and bone fixation materials for instance as bone screws or plates. Within a certain time span after surgery, they degrade and are completely suitable to medical functions [1-2, 7-8].

However, several problems need to be settled for the application of Mg to the biomedical field, such as poor corrosion resistance in chloride containing solutions and pittings especially in body fluid condition.

1.1.4 Titanium (Ti) and its alloys: Ti and its alloys possess low modulus varying from 110 to 55 GPa [1]. Commercially pure Ti and Ti–6Al–4V are most commonly used titanium materials for implant applications. High corrosion resistance and excellent biocompatibility increases its suitability for biomedical industry. The mechanical strength of the Ti and its alloys is very close to that of 316 L SS, and its density is 55% less than steel. The applications cover joint replacement parts for hip, dental implants, knee, elbow, spine, shoulder etc. Although titanium and its alloys mainly Ti6Al4V have an excellent corrosion resistance and biocompatibility, long term use leads to release of Al and V ions. Both vanadium and aluminum ions released from the Ti6Al4V alloy are found to be cause long-term health problems, like Alzheimer disease etc [1]. Toxicity of vanadium has also been reported, both in the elemental state and oxides V_2O_5, which are present at the surface. Bioinertness of Ti also restricts its use [1].

Beside Cp-Ti and Ti6Al4V, β-titanium alloys such as Ti-Ta alloys; Ti-Mo alloys; Ti-Nb and Ti-Ni shape memory alloys are very much attracted as bioimplants [1, 9]. These alloys exhibit high corrosion resistance and biocompatibility. Ti-Ta alloys have much

lower modulus and a good combination of high strength and low modulus. They have the great potential to become new candidates for biomedical applications. Adding Zr to the Ti alloy lowers the Young's modulus and other mechanical properties suitable for biomedical applications [1].

1.1.5 Shape memory alloys: Nickel-titanium (Ni-Ti) shape memory alloys have been recently discovered as a very important bone implant due to its excellent mechanical properties, good corrosion resistance, high biocompatibility, special pseudoelasticity and shape as well as volume memory effect. Its porous structure permits the ingrowth of new-bone tissue along with the transport of body fluids. Moreover, by obtaining different porosity through controlling the processing parameters, the elastic modulus of the final porous Ni–Ti could be adjusted and matched with that of human bone [9]

1.1.6 Ti-Ha metal matrix composite: Recent advancement in this field of biomaterials which has caught the eye of researcher's is Ti-Ha metal matrix composite. The excellent biocompatibility and bioactivity of Ha is blended with the inert and superior mechanical properties of titanium to get a composite with enhanced biocompatibility, bioactivity and favorable mechanical properties [4, 10-11]. This composite has been reported to be non-toxic and highly bioactive. The porous nature facilitates the bone in growth and better osseointegration. The *in vitro* results in simulated body fluid (SBF) have shown dense hydroxyapatite particles deposited on the implant [3-5]. Also it has been found that tensile strength, Young's modulus decreases with increase in volume fraction of Ha. This composite has also been found to be thermodynamically and electrochemically stable in the body environment [12].

The present research work deals with deals with the processing of Ti-Ha composite and its characterization as biomaterial. The composite is prepared by powder metallurgy technique. The composite powder is then compacted, sintered and its bioactivity is assessed in SBF.

Chapter 2: Literature Review

2.1 International Status: A lot of work has been done internationally in this field. Few noted works related to this project are listed below.

Wen Shi et. al, 2002, varied the volume of Ha from 3% wt. to 30% wt. and reported that Ha distribution up to 15% wt. of Ha had no defect. Non-uniformity appeared from above 22% wt. The tensile strength for 22% wt. was reported to be 140 Mpa and decreased as Ha content increased. Crystalline apatite was formed when samples were soaked in SBF for 14 days [13]

C. Q. Ning et. al, 2004; studied the processing of bioactive material using Ti, Ha and bioglass. The bioglass was kept fixed at 10% by volume while Ha was varied from 20 to 60% by volume. It was reported that the optimum temperature for sintering the Ti-Ha composite was 1200^{o} C and Ha did not decompose at this temperature. Ti at 1200^{o} C remained in its h.c.p. structure (α-Ti) [14].

Congqin Ning et. al, 2008; prepared Ti-Ha composite by ball milling and sintering. The polished samples were immersed in SBF as well as transplanted in to a rabbit. Apatite particles were formed on the sample with higher Ti content. However the gap in bone formation was observed with increasing Ti. A thin film of bone had developed after one month in the pores of the sample. The thickness of the bone increased after 6 months. However no bonding at the interface was reported [3].

G. Zhao et. al, 2012; studied plasma sprayed Ti-Ha biocomposite. Ha content was varied from 80% wt. to 20% wt. It was found that ball milled powders consisted of spherical Ti-Ha composite particles. Microhardness, modulus of elasticity and bond strength increased with increasing Ti. The elasticity of composite containing 80% wt. Ha was 52.1 GPa. Also the composite showed apatite formation except for the composite containing 20% wt. Ha [15].

Chu Chenglin et. al, 1999; processed a functionally graded Ti-Ha composite. Decline in density with increase in Ha concentration was reported. The relative density was found to be

maximum in the two pure component regions. Hardness increased up to the region with 20% volume Ha. However the hardness decreased in the 40% volume Ha region to 80% volume Ha region due to decrease in density. Young's modulus was also observed to decrease in the 40 – 80% volume Ha regions [16].

S. Salman et. al, 2009; reported that high densification regime was observed after sintering the Ti-Ha composite at 1300^{o} C whereas sample sintered at 1000^{0} C showed poor densification when characterized [17].

C.Q Ning et. al, 2002; studied the milling of Ti and Ha powders in 1:1 ratio and sintering at 1200^{o} C. Many globular apatite particles had formed on the pores of the sample on immersion of the sample in SBF during bioactivity test. The pH increased gradually throughout the immersion process [3]

Shahrjerdi et. al, 2011; prepared Ti-Ha composite by powder metallurgy with varying Ti, Ha content . It was observed that hardness increased with increase in Ha but for 25 - 70% wt. Ha compositions, lower density resulted in the decrease of hardness. [10]

Q.Chang et. al, 2011, synthesized Ti-Ha composite by powder metallurgy. It was reported that Ha was thermally stable at 1000^{o} C and no decomposition of Ha occurred. It was also found that after immersion in SBF for 1 week, tiny apatite particles were formed on the surface of the samples. A dramatic increase in the precipitate was observed after 5 weeks [5].

Jung G Lee et. al; 2010; studied the effect of milling on the Ti-Ha composite. TiO_2 containing both rutile and anatase phase was mixed with Ha. Ball milling speed and the ball milling time was varied. It was found that on increasing the ball milling time, anatase phase transformed to rutile phase. It was also found that phase transformation increased with decrease in Ha content [11].

A Siddhartan et. al, 2010; used microwave to sinter the titania-hydroxyapatite composite. A layer of Ha coating was observed on the Ti-Ha composite surface without any delamination.

However oxide had formed on the surface. In the bioactivity test it was found that Ha particles had formed on the grain boundaries of oxide and over the Ha particles. The samples also showed better cell adhesion and cell spreading [18].

Q Chang et. al, 2010; blended Ti, Fe and Ha. The samples were ball milled and sintered at 1000^{o} C. It was observed that on adding Ti-Fe the average density of the composite decreases. The hardness also decreases with increase in Ti-Fe concentration. It was further concluded that the presence of Fe reduces the decomposition of Ha [19].

Anawati et. al, 2013; reported that the corrosion potential of Ti-Ha composite increased and stabilized the surface leading to passivation. This showed high corrosion resistance of the Ti-Ha composite. SBF test showed globular particles after 2 day immersion in SBF. Pure Ti sample did not show any apatite on its surface on immersion in SBF [12].

Wenxiu Que et. al, 2008; prepared a biocomposite by mixing the TiO_2 and Ha particles. The mixed powders were ball milled and spark plasma sintered. It was reported that hardness and modulus of the composite are functions of sintering temperature. Both modulus and hardness increases with increase in sintering temperature. Nano sized flaky crystallite of apatite had formed on nano-composite compact [20].

X. Zhou et. al, 2012; prepared Ti composite from Ti powders and Ha was cold sprayed over it. It was reported that 20% wt. Ha-Ti composite coating shows more corrosion current and thus poor corrosion resistance [21].

Xuebin Zheng et. al, 2000; processed Ti-Ha composite by ball milling. Ti6Al4V was used as substrate for plasma spraying. Polished specimens were soaked in SBF. It was reported that the bond strength of the coating increases on adding Ti to Ha. Adhesion increased on further increasing the Ti content. The cohesive strength of the particles in the coating also increases on increasing the Ti content. Apatite coating was observed even after I day of coating [22].

Chenglin Chu et. al, 2006; prepared functionally graded Ti-Ha composite by powder metallurgy technique. It was observed that new bone had developed after 8 weeks of implantation. Bone tissues were formed after 28 months. It was concluded that osseointegration and osseoinduction of functionally graded composite is more than that of pure Ti, and that the bonding strength increases slowly after different implanting time while that of functionally graded material increases at much faster rates [23].

2.2 National status: Very few researchers have worked in this field. However detailed and systematic study in this area is required.

Chapter 3: Materials and Methods

Pure Cp-Titanium powder (supplied by Himedia) was mixed with pure Ha powder. The powders were mixed in varying % wt. ratio and coded as shown in Table 1.

Table 1: Sample code and composition

Sample code	Titanium (Ti) (% wt.)	Hydroxyapatite (Ha) (% wt.)
Ti	100	0
Ti10	90	10
Ti15	85	15

3.1 Sample preparation

The Ti and Ha powders were mixed according to their respective % wt. as shown in Table 1 and then ball milled in a planetary ball mill machine (Fritsch Planetary Ball Mill – Puluerisette 5) for 8 h. Ethanol was used as wetting media. Ball milling was done using stainless steel vial and stainless steel balls and the ball to powder mass ratio 20:1 was maintained. The ball milling was done at 300 rpm and milling was done in a cycle of 15 min and was put on rest for next 15 min. This cycle was continued till 8 h of effective milling time. The milled powders were compacted in uniaxial single action (SOILLAB, Delhi) hydraulic compaction machine, using a 15 mm diameter die and using 10 ton load. Zinc stearate was used as lubricant. The green compact was then sintered in muffle furnace (SEMAG Industries) at 900^{o}C for 30 min in normal atmosphere. The heating rate was set as 200^{o}C/min.

3.2 Sample characterization

The sintered samples were polished on grade 1 to 4 abrasive silicon carbide paper. Polished samples were cleaned in distilled water and ultrasonicated in acetone for 15 min. The as milled and sintered samples were characterized using scanning electron microscope (SEM), (JEOL JSM – 6480LV) and XRD (PANalytical - Xpert 3040Y00) for morphology and phase contamination. The scanning range for XRD was between 20^{o} - 60^{o} with a step size of $3\ ^{o}$/min.

3.3 Density measurement

The polished and ultrasonicated samples were immersed in a measuring cylinder containing distilled water. The corresponding change in the volume of the water was measured. The densities of the samples were calculated using Archimedes' principle. According to the Archimedes principle, the increase in volume of water corresponded to the volume of the immersed sample. The density of the samples was calculated from the fundamental formula, density = mass/volume.

3.4 *In-vitro* bioactivity study in SBF

The polished samples were ultrasonically cleaned in distilled water and then acetone for 15 min and dried. The samples were soaked in freshly prepared SBF for 2 weeks. The SBF is a solution with ion concentration close to that of human blood plasma and is kept under mild conditions of pH and identical physiological temperature. Table 2 shows the amount of reagents required to prepare 1 liter of SBF [24].

Table 2: Reagents for the preparation of one liter SBF

Reagents	Amount
NaCl	8.035g
$NaHCO_3$	0.355g
KCl	0.225g
$K_2HPO_4.3H_2O$	0.231g
$MgCl_2.6H_2O$	0.311g
1.0M HCl	39-44 ml
$CaCl_2$	0.292g
Na_2So_4	0.292g
Tris	6.118g

SBF was prepared by following Kokubo's protocol [24]. The pH of the finally prepared sample was adjusted to 7.42 by adding 1.0 M HCl. SBF was stored in clean container in refrigerator at 4^{o}C. Each sample was kept in 50 ml plastic falcon tube containing 50 ml SBF. The falcon tube was then kept in a water bath at 37^{o}C. After each week the samples were taken out, washed with distilled water, dried and characterized using SEM and XRD for apatite morphology.

Chapter 4: Results

4.1 Density Measurement

The densities of the samples were calculated by Archimedes' principle. Table 3 shows the results of the density measurement by Archimedes' principle as well as by theoretical density calculation. The results showed that the density decreased with increase in hydroxyapatite concentration. Relative density of Ti10 was found to be 99% whereas for Ti15, the relative density was found to be 94% for Ti15 with respect to ball milled pure Ti sample.

Sample Code	Density by Archimedes Principle (g/cc)	Theoretical Density (g/cc)
Ti	3.233	3.267
Ti10	3.230	3.169
Ti15	3.060	3.09

Table 3: Density measurement by Archimedes principle

4.2 XRD analysis

4.2.1 Powder composite characterization

Fig. 1 shows the phase composition of milled pure Cp-Ti powder. The result for the pure Cp-Ti powder milled for 4 h shows that the peak generally corresponds to Ti peaks (JCPDS ICDD PDF: 05-0682). No oxide was formed after 4 h of milling. The XRD pattern of Cp-Ti after 8 h of milling showed decrease in intensity of the Ti peaks. The peak width of the 8 h ball milled Cp-Ti powder increased indicating refinement of the crystallite size. No oxide formation or any contaminations from the vials were observed after 8 h of ball milling. Slight shift in peaks were observed which was due to strain imposed on the powder due to ball milling.

Fig. 2 shows the XRD pattern of titanium – hydroxyapatite (Ti-Ha) composite mixed in the % wt. ratio of 90:10 (Ti10). XRD pattern after 4 h of ball milling exhibited both Ti

and Ha (JCPDS ICDD PDF: 09-0432) peaks. No contaminations from the vials during ball milling were observed. XRD pattern of the composite after 8 h milling time shows a decrease in the intensity of the Ti and Ha peaks. The Ti peaks showed slight broadening after 8 h of ball milling than 4 h of ball milling indicating the refinement of the particle size. No oxide formation and contamination were observed after 8 h of ball milling.

Fig. 3 shows the XRD pattern of the Ti-Ha composite with 85:15 % wt. Ti, Ha ratio (Ti15). XRD pattern after 4 h of ball milling exhibited no contamination from the vials during ball milling. Ti phase was dominant after 4 h ball milling time. XRD pattern of 8 h ball milled composite showed a decrease in the intensity of Ti peak. This decrease in the intensity of Ti peaks shows a refinement of crystal size. The peak broadening with increase in ball milling time indicates a decrease in crystallite size. Ha intensity decreased drastically after 8 h of ball milling indicating fusion of Ha in the composite. No oxide formation and contamination after 8 h ball milling was observed.

4.2.2 Sintered composite characterization

Fig. 4 shows the phase analysis of the compacted, sintered and polished samples with different Ti-Ha % wt. ratio. Sintering was done at 900^{o}C in muffle furnace in normal atmosphere. The green compacts were put inside ceramic crucibles and covered with the ceramic lid. The XRD pattern of sintered pure Cp-Ti showed that sintering at high temperature in normal atmosphere has led to formation of oxide peaks of Ti. Titanium has oxidized to its oxide form TiO_2 (JCPDS ICDD PDF: 21-1276). TiO_2 existed in its rutile phase. Sintering of Ti10 and Ti15 has led to the oxidation of TiO_2. At 900^{o}C, reaction between Ti and Ha has led to the formation of $CaTiO_3$ (JCPDS ICDD PDF: 22-153).

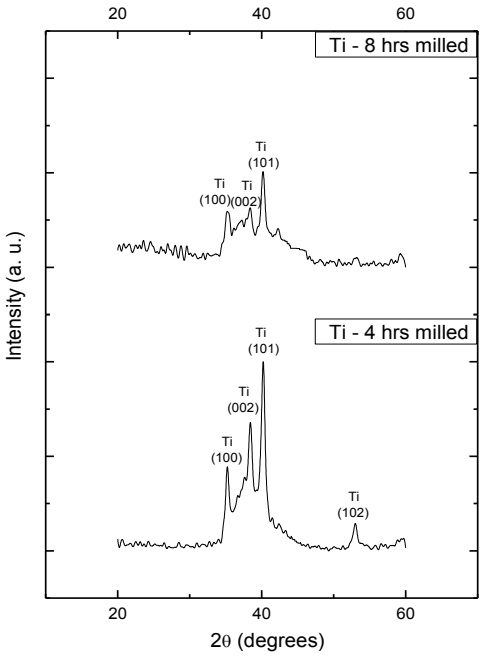

Fig. 1: XRD pattern of ball milled pure Cp-Ti powder for various time intervals.

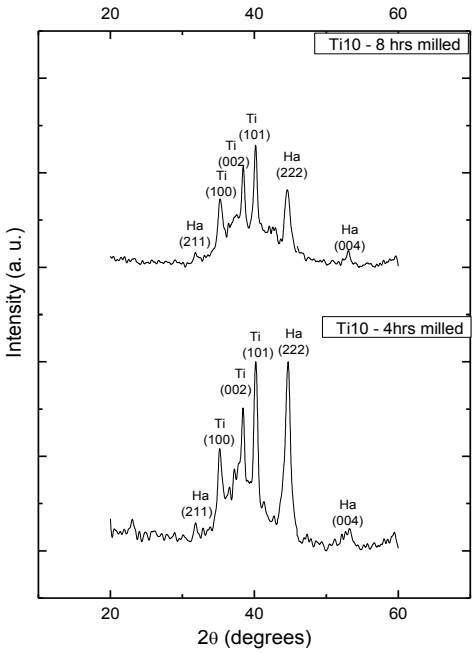

Fig. 2: XRD pattern of ball milled Ti10 powder for various time interval.

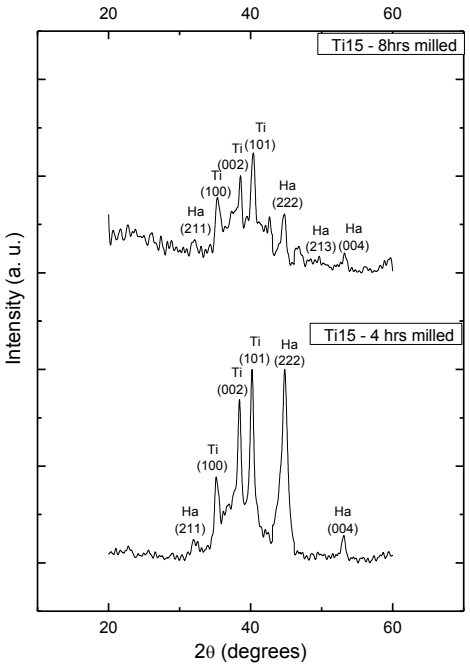

Fig. 3: XRD pattern of ball milled Ti15 powder for various time intervals.

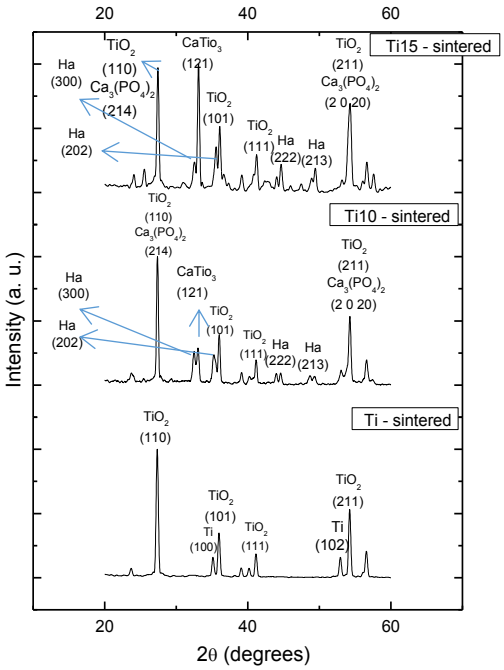

Fig. 4: XRD pattern of compacted and sintered samples.

Formation of $Ca_3(PO_4)_2$ (JCPDS ICDD PDF: 09-0169) phase was observed on the samples. Oxidation of Ti into TiO_2 was observed (Fig. 4). Peaks of Ha were observed after sintering at 900^oC, which showed the partial decomposition of Ha at this temperature. XRD pattern of Ti15 composite shows peaks of TiO_2, $CaTiO_3$ and Ha (Fig. 4). The intensity of TiO_2 and $CaTiO_3$ peaks increased showing that with increase in Ha concentration, the oxidation increases and more reaction took place between Ti and Ha. The peaks of $Ca_3(PO_4)_2$ also increased showing more decomposition of Ha.

4.2.3. In-vitro bioactivity study in SBF

Fig. 5 shows the XRD pattern of the sintered pure Cp-Ti sample soaked in SBF for 1 and 2 weeks. XRD plot of the sample soaked in SBF for 1 week shows the formation of apatite after 1 week immersing in SBF. XRD pattern of the 2 weeks soaked sample showed that the intensity of Ha peak increased. The intensity of the TiO_2 peak decreased after 2 weeks indicating that more Ha has formed all over sample. Phase of CaO (JCPDS ICDD PDF: 04-0777) was observed after 2 weeks of soaking. Phase analysis of the pure Cp-Ti sample before immersion (Fig. 4) shows the presence of TiO_2. The intensity of TiO_2 decreased with soaking time indicating formation of apatite on the sample surface.

Fig. 6 shows the XRD pattern of Ti10 samples soaked in SBF for 1 and 2 weeks. XRD peaks of the 1 week soaked sample showed the phases of Ha, $Ca_3(PO_4)_2$ and CaO. The intensity of these peaks increased with soaking time. Increased peak showed a uniform deposition of Ha on the sample. No TiO_2 peak was observed as in the case of pure Ti powder sample (Fig. 5). XRD analysis of the Ti10 samples before soaking (Fig. 4) showed the presence of TiO_2 which was now coated with Ha.

Fig. 7 shows the XRD pattern of Ti15 composite soaked in SBF for 1 and 2 weeks. XRD pattern of Ti15 samples soaked in SBF for 1 week shows the presence of Ha, $Ca_3(PO_4)_2$ and CaO phases. With increase in soaking time the intensity of these phases increased considerably indicating increase in the deposition of Ha on the sample. XRD analysis of

samples before coating showed the presence of TiO_2 (Fig. 4). However no such TiO_2 peaks were found after soaking in SBF.

A comparative study of all the Ti, Ti10 and Ti15 samples soaked in SBF for different time interval showed that the hydroxyapatite formation was more in Ti15 samples and least in pure Ti sample. The intensity and distribution of Ha increased with increased in Ha content in the sample. With increasing time the apatite layer grew thicker as shown in SEM micrograph (Fig. 10)

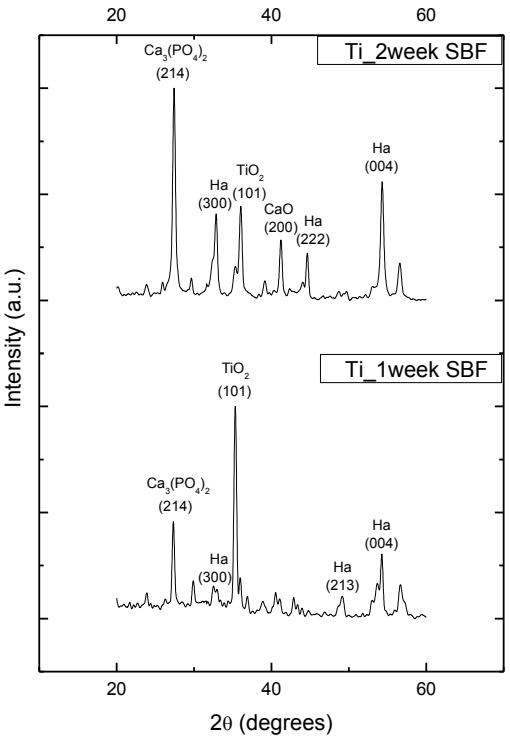

Fig. 5: XRD pattern of sintered pure Cp-Ti soaked in SBF for 1 and 2 weeks.

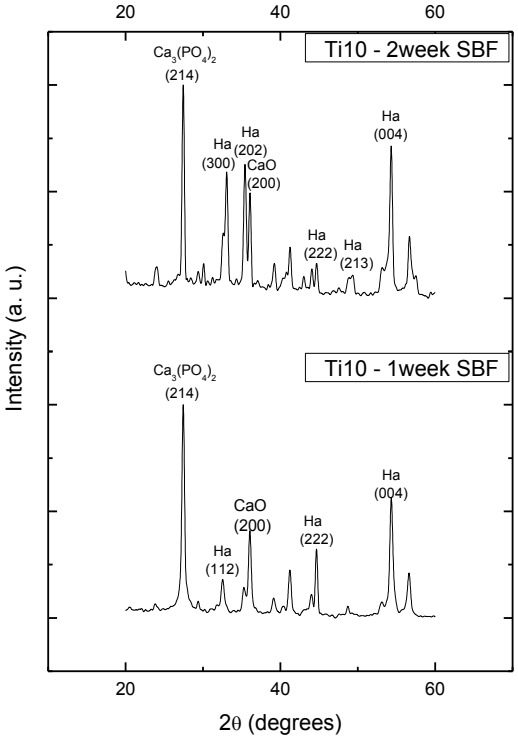

Fig. 6: XRD pattern of sintered Ti10 composite soaked in SBF for 1 and 2 weeks.

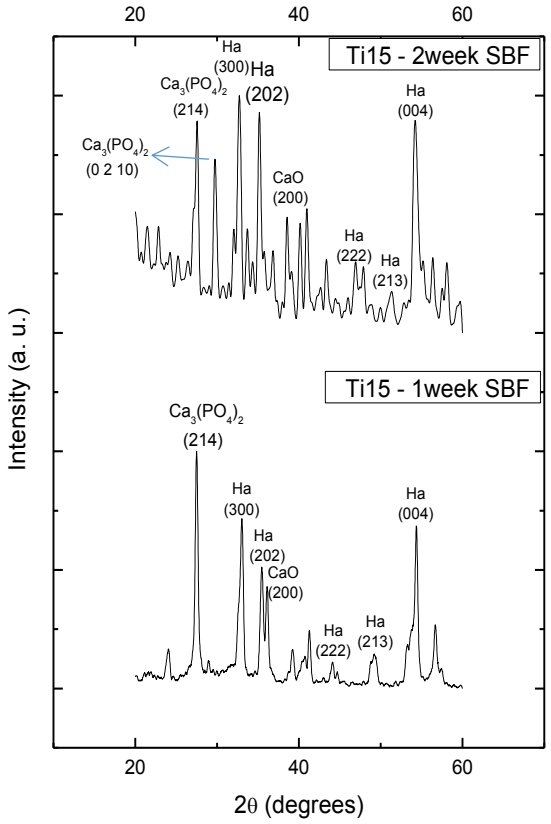

Fig. 7: XRD pattern of sintered Ti15 composite soaked in SBF for 1 and 2 weeks.

4.3 SEM Characterization

4.3.1. Powder composite

Fig. 8 shows the shows the SEM micrographs for 8 h ball milled Ti-Ha composite powder with different Ti/Ha % wt. ratios. Fig. 8a shows the microstructure of 8 h ball milled pure Cp-Ti powder where the particle size of the pure titanium powder was almost uniform after the milling. The average sizes of the particles from the micrographs were found to be less than 10 µm. The particles were irregularly plate shaped. Fig. 8b shows the microstructure of the Ti10 composite. The average sizes of the particles are

comparatively more than those of pure titanium. Fig. 8c shows the microstructure of the Ti15 milled powder composite. The powder composite showed a more equiaxed particle structure. The size was more uniform and larger when compared to other composition.

4.3.2. Sintered composite

The sintered composite samples were polished on silicon carbide abrasive paper, ultrasonicated in acetone and then observed under SEM. Fig. 9a shows the microstructure of pure Cp-Ti sample. The bright regions shows the extensive oxide layer formed on the sample as exhibited in the XRD analysis (Fig. 4). Small pores were also observed in the microstructure. Fig. 9b shows the microstructure of Ti10 composite. With addition of percent of Ha, the porosity increased. The bright regions also increased in the microstructure showing an increase in oxide formation. Similar structure was also observed in Ti15 composite. Fig. 9c shows a more porous structure for Ti15 composite when compared to other compositions. Porosity increased with increase in Ha concentration. Fig. 9d shows the cross section of the Ti15 composite. Spherically sized pores, uniformly distributed throughout the structure can be seen.

4.3.3. In-vitro bioactivity study in SBF

Fig. 10 shows the SEM micrograph of samples with different Ti-Ha % wt. ratio soaked in SBF for 1 and 2 weeks. Fig. 10a shows the microstructure of pure Ti soaked in SBF for 1 week. It was observed that globular apatite particles have been deposited on the sample and more globular apatite was deposited after 2 weeks of immersion (Fig. 10b). Fig. 10c shows the surface of Ti10 samples where more globular apatite was observed when compared to pure Cp-Ti samples. Increasing the immersion time leads to the nucleation of more apatite particles. Figure also shows the flaky structures of $Ca_3(PO_4)_2$ as exhibited in XRD analysis (Fig. 6). Fig. 10e shows the micrograph of Ti15 samples. The surface of Ti15 is covered with more globular structure as compared to Ti and Ti10 samples. Also Ti15 sample soaked for 2 weeks showed more apatite nucleated. A thick layer of apatite can be seen on Ti15 surface soaked in SBF for 2 weeks of immersion (Fig. 10f). With the increase of immersion time, more apatite deposits and their size grew gradually forming dense apatite layer.

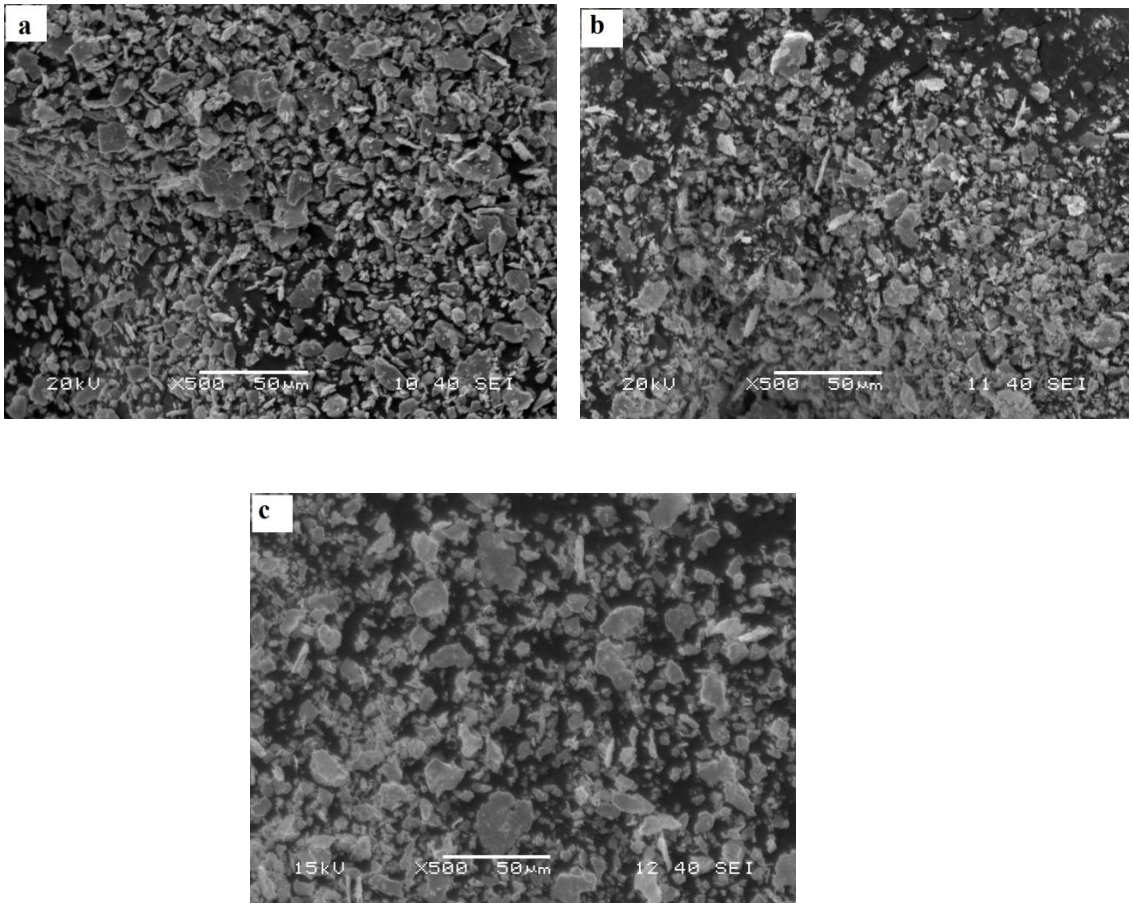

Fig. 8: SEM micrographs of 8 h ball milled composite powder. (a) Pure Cp-Ti powder (b) Ti10 powder (c) Ti15 powder

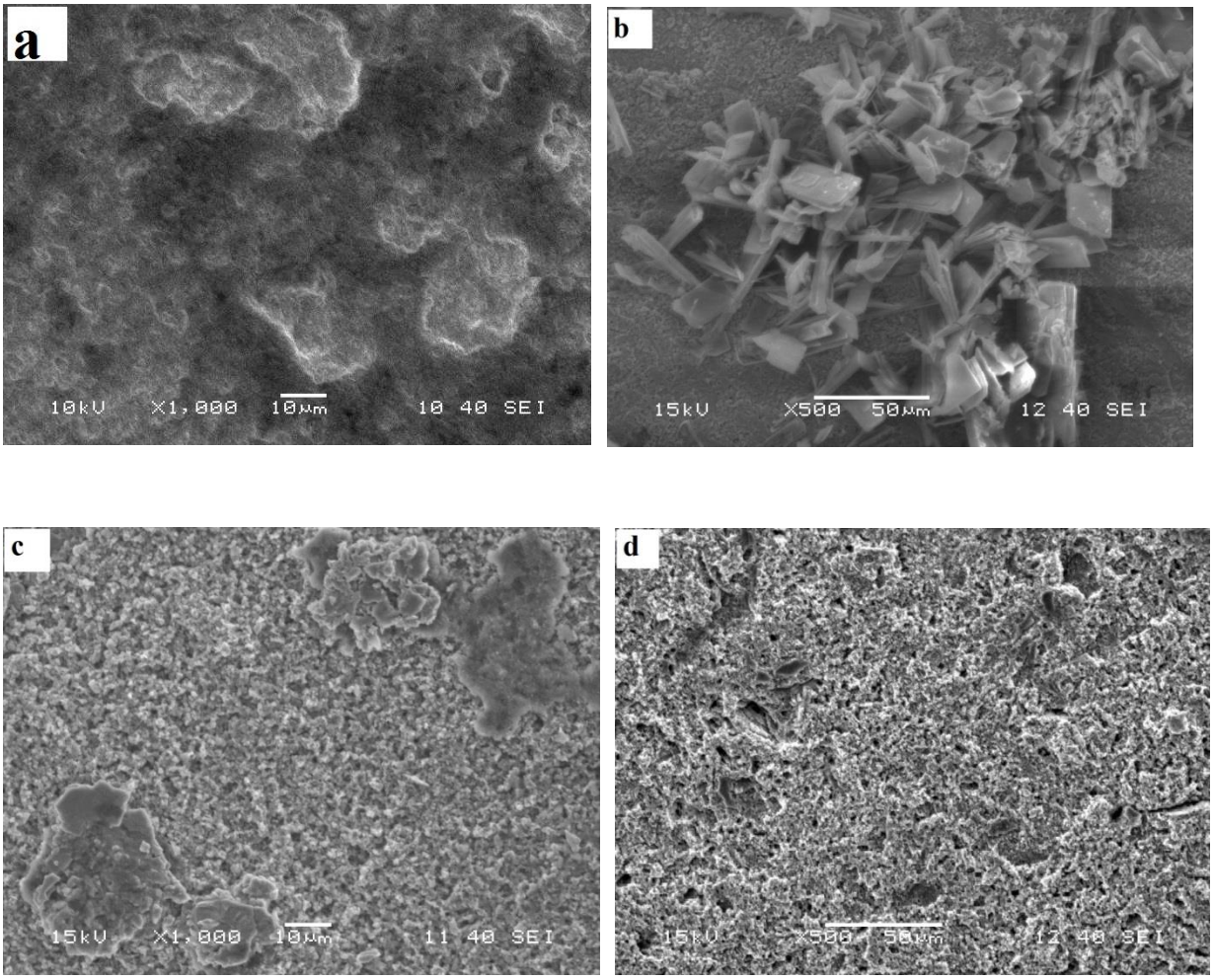

Fig. 9: SEM micrograph of polished and sintered composite. (a) pure Cp-Ti (b) Ti10 composite (c) Ti15 composite (d) cross section of Ti15 composite

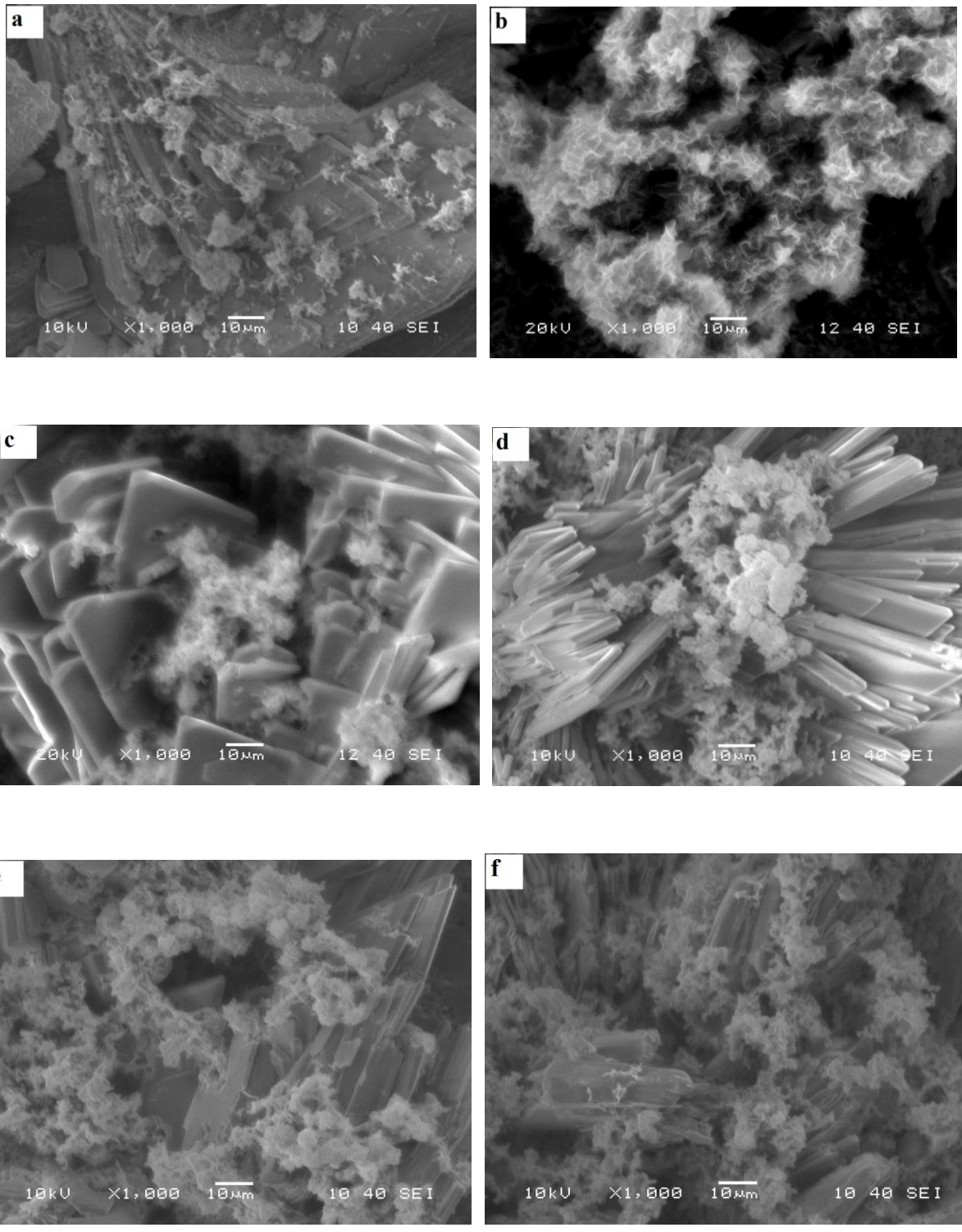

Fig. 10: SEM micrographs of ball milled and sintered samples soaked in SBF. (a) Pure Cp-Ti, for one week (b) pure Cp-Ti, for two weeks (c) Ti10, for one week (d) Ti10, for two weeks (e) Ti15, for one week (f) Ti15, for two weeks.

Chapter 5: Discussion

5. Discussion

5.1. Powder composite

High energy ball milling is used to mechanically blend two or more powder materials into a homogenous mixture of nano and sub micrometer range. In the present study Ti and Ha of various % wt. were mixed and ball milled to form a Ti-Ha composite and their bioactivity was studied. High ball milling resulted in the plastic deformation of Ti particles which resulted in reduction in their crystallite size. During ball milling, repeated cold welding and fracture takes place. This is also evidenced by XRD pattern as the intensity of Ti peaks was reduced. Broadening of Ti peaks was observed for increase in milling time (Fig. 1). However some larger particles were depicted in the micrograph. This is due to agglomeration of particles as a result of ball milling [25].

On addition of Ha to Ti, the composite particles were found to be bigger than those of pure Ti ball milled powder and spherical in size. Since Ha is brittle material, it was easily ground to smaller particles. These fine Ha particles have very high surface energy, they tend to stick to Ti particles and results in the formation of composite powder. The particle size of the composite Ti15 (Fig. 8c) were larger than those of Ti10 (Fig. 8b) particles due to above mention mechanism. More Ha content resulted in the formation of larger particles.

The XRD pattern of ball milled Ti-Ha shows no phase other than Ti and Ha (Fig. 2-3). This is because Ha do not decompose at low temperature. It is highly stable at room temperature. Also no oxidation of Ti takes place at this temperature. The temperature rise during milling is not sufficient to carry out such reactions. Also milling was carried out in presence of a wetting media to minimize the increase in temperature during ball milling. The intensity both Ti and Ha peaks decreased due to refinement in structure.

5.2. Sintered composite

D. J. Green et. al, defined sintering as a process involving heating a powder assemblage or other porous structures below their melting point. It produces materials in a robust and useful form. The porous structure usually undergoes densification and strengthening, as well

as developing other required functions [26]. This process is generally used for the materials having high melting point. Ti has a melting point of 1668^{o}C and that of Ha is 1760^{o}C. In this study sintering of Ti-Ha composite was done at 900^{o}C in muffle furnace. XRD pattern of pure Ti powder (Fig. 4) shows peaks of TiO_2. High temperature sintering has resulted in the oxidation of Ti metal. The oxidation could have been as a result of high temperature sintering in normal atmosphere. As a well-known fact Ti undergoes an allotropic transformation at about 890^{o}C which may have resulted in the oxidation of Ti to TiO_2. Microstructure of sintered Ti shows very less pores as the sintering resulted in grain growth which has further resulted in greater density of the specimen (Fig. 9a).

High temperature sintering of the Ti-Ha composite has initiated reaction between Ti and Ha. XRD pattern shows the presence of $CaTiO_3$ phase. Phase of $Ca_3(PO_4)_2$ was found due to the decomposition of Ha (Fig. 4). The decomposition of Ha could have resulted in to $Ca_3(PO_4)_2$, and CaO. The decomposition of Ha could have been initiated by the presence of TiO_2 [15]. The samples with Ha content depict large pores which could be due to the dissolution of CaO. The porous structure increases with increase in Ha content. More Ha content would have led to the more decomposition and hence more dissolution of CaO (Fig. 9 (b-d)). No Ti phase in composite containing Ha could be observed because Ti could have either oxidized or reacted with the decomposition product of Ha to give a new phase, $CaTiO_3$.

The density of the Ti, Ti10 and Ti15 was found to be 3.233, 3.230 and 3.06 g/cc respectively (Table 3). The decrease in the density with addition of Ha could be a result of dissolution of CaO, a decomposition product of Ha. The density of the composite was less than that of Ti (4.51 g/cc). The volume fraction of pores could be calculated from this data. The volume fraction of pores in Ti, Ti10 and Ti15 were found to be 28.31%, 28.38% and 32.15% respectively, which has accounted for the porous structure of the Ha containing Ti composite. This porous structure would enhance osseointegration when implanted in-vivo.

5.3. In-vitro bioactivity study in SBF

SBF is a laboratory developed fluid which has similar inorganic ion concentration as that of human extracellular fluid, in order to initiate the development of apatite on bioactive

materials in-vitro. SBF is used to evaluate the bioactivity of the materials for bone tissues in-vitro. Though SBF is metastable calcium phosphate solution, it can be stored for almost two months without any precipitate formation. Hence if apatite has formed on surface of a material, it is only due to the interaction between the material and SBF. Hydroxyapatite is formed only if the material is bioactive when immersed in SBF. This apatite forming process can be interpreted in terms of the surface charge. The titanium composite is initially negatively charged, and hence combines with positively charged calcium ions in SBF to form a calcium titanate. As the calcium ions are accumulated, the surface is positively charged and hence combines with negatively charged phosphate ions to form an amorphous calcium phosphate with low Ca/P ratio (~1.48). This phase is metastable and hence eventually transforms into crystalline bone-like apatite with Ca/P ratio almost similar to that of bone (~1.66). The apatite globules were much larger and densely packed when compared to all other conditions.

Microstructure of the composite soaked in SBF for 1 and 2 weeks shows the globular apatite formed on the surface (Fig. 10). Ti15 shows the maximum apatite grown on its surface (Fig. 10 (e-f)). $Ca_3 (PO_4)_2$ is one of important biomaterial owing to its high bioactivity [15]. This may be a possible reason to induce apatite formation on the surface of Ti10 and Ti15.

The existence of CaO could also induce apatite nucleation. Supersaturation of SBF with respect to calcium phosphate will increase which will lead to decrease in the free energy for the formation of embryo with critical size, which favors nucleation and growth of apatite [4]. TiO_2 reacts with water to form Ti-OH. This Ti-OH on the surface may provide specific favorable site for apatite formation due to lower free energy for apatite nucleation. Fig. 10b, Fig. 10d, Fig. 10f shows increased apatite coated on the surface with increase in time. Once the apatite nuclei have formed, they can grow over time by consuming the calcium and phosphate ions from SBF. This is shown by the increase in diffraction intensity of immersed sample after 2 weeks (Fig. 5-7).

Chapter 6: conclusion

Ti-Ha composite was successfully prepared by powder metallurgical route using a high energy ball milling and subsequent sintering. Density and bioactivity of the sintered samples were assessed in simulated body fluid. From the study the following conclusions are drawn.

1) The sintered sample showed more porous structure with increase in Ha content. The volume fraction of pores was found to be more in Ti15 composite.

2) Sintering at 900 ^{o}C resulted in partial decomposition of Ha. At this temperature, reaction between Ti and Ha occurred resulting in the formation of $CaTiO_3$ which initiates more apatite formation. $Ca_3(PO_4)_2$ and TiO_2 were detected from XRD analysis which favors apatite formation.

3) The composite containing hydroxyapatite showed better bioactivity than pure Cp-Ti and the hydroxyapatite deposition increased with increase in Ha content when immersed in SBF for the same time period (1 week).

References

References

1. **M. Geetha, A.K. Singh, R. Asokamani and A.K. Gogia.** *Ti based biomaterials, the ultimate choice for orthopaedic implants – A review*. (2009), Progress in Materials Science, Vol. 54, pp. 397–425.

2. **S. R. Paital and N. B. Dahotre.** *Calcium phosphate coatings for bio-implant applications: Materials, performance.* (2009), Materials Science and Engineering R, Vol. 6, pp. 1-70.

3. **C. Ning and Y. Zhoub.** *Correlations between the in vitro and in vivo bioactivity of the Ti/HA composites fabricated by a powder metallurgy method*. (2008), Acta Biomaterialia, Vol. 4, pp. 1944-1952.

4. **C.Q. Ning and Y. Zhou**. *In vitro bioactivity of a biocomposite fabricated from HA and Ti powders by powder metallurgy method.* (2002), Biomaterials, Vol. 23, pp. 2909-2915.

5. **Q. Chang, H.Q. Ru, D.L. Chen, X.Y. Yue, L. Yu and C.P. Zhang.** *An in-vitro Investigation of Iron-Containing Hydroxyapatite/Titanium Composites.* (2011), J. Mater. Sci. Technol, Vol. 27, pp. 546-552.

6. **E.J. Giordani, V.A. Guimaraes, T.B. Pinto and I. Ferreira.** *Effect of precipitates on the corrosion–fatigue crack initiation of ISO-5832-9 stainless steel biomaterial*. 2004, International Journal of Fatigue, Vol. 26, pp. 1129-1136.

7. **S. Hong-fei, L. Cheng-jie and F. Wen-bin.** *Corrosion behavior of extrusion-drawn pure Mg wire immersed in simulative body fluid.* (2011), Trans. nonferrous Met. Soc. China, Vol. 21, pp. 258-261.

8. **X. Cui, Y. Yang, E. Liu, G. Jin, J. Zhong and Q. Li.** *Corrosion behaviors in physiological solution of cerium conversion coatings on AZ31 magnesium alloy.* (2011), Applied Surface Science, Vol. 257, pp. 9703-9709.

9. **C.L. Chu, R.M. Wang, T. Hu, L.H. Yin , Y.P. Pu , P.H. Lin , S.L. Wu, C.Y. Chung, K.W.K. Yeung and P. K. Chu.** *Surface structure and biomedical properties of chemically polished and electropolished NiTi shape memory alloys.* (2008), Materials Science and Engineering C, Vol. 28, pp. 1430-1434.

10. **A. Shahrjerdi, F. Mustapha, M. Bayat, S. M. Sapuan and D. L. A. Majid.** *Fabrication of functionally graded Hydroxyapatite-Titanium by applying optimal sintering procedure and powder metallurgy*. (2011), International Journal of the Physical Sciences, Vol. 6, pp. 2258-2267.

11. **J. G. Lee, S.M. Hong, J.J. Park, M.K. Lee, S.J. Hong, U.H. Joo and C.K. Rhee**. *High energy ball-mill behavior of titania + hydroxyapatite composite nano-powders*. (2010), Materials Characterization, Vol. 61, pp. 1290-1293.

12. **Anawati, H. Tanigawa, H. Asoh, T. Ohno, M. Kubota and S. Onoa.** *Electrochemical corrosion and bioactivity of titanium–hydroxyapatite composites prepared by spark plasma sintering.* (2013), Corrosion Science, Vol. 70, pp. 212-220.

13. **W. Shi, A. Kamiya, J. Zhu and A. Watazu.** *Properties of titanium biomaterial fabricated by sinter-bonding of titanium/hydroxyapatite composite surface-coated layer to pure bulk titanium.* (2002), Materials Science and Engineering: A, Vol. 337, pp. 104 - 109.

14. **C.Q. Ning and Y. Zhou.** *On the microstructure of biocomposites sintered from Ti,HA and bioactive glass.* (2004), Biomaterials, Vol. 25, pp. 3379-3387.

15. **G. Zhao, L. Xia, G. Wen, L. Song, X. Wang and K. Wu.** *Microstructure and properties of plasma-sprayed bio-coatings on a low-modulus titanium alloy from milled HA/Ti powders.* (2012), Surface and Coatings Technology, Vol. 206, pp. 4711-4719.

16. **C. Chenglin, Z. Jingchuan, Y. Zhongda and W. Shidong**. *Hydroxyapatite–Ti functionally graded biomaterial fabricated by powder metallurgy.* (1999), Materials Science and Engineering: A, Vol. 271, pp. 95-100.

17. **S. Salman, O. Gunduz, S. Yilmaz, M.L. Öveçoğlu, Robert L. Snyder, S. Agathopoulos and F.N. Oktar.** *Sintering effect on mechanical properties of composites of natural hydroxyapatites and titanium.* (2009), Ceramics International, Vol. 35, pp. 2965-2971.

18. **A. Siddharthan, T.S. Sampath Kumar and S.K. Seshadri.** *In situ composite coating of titania–hydroxyapatite on commercially pure titanium by microwave processing.* (2010), Surface and Coatings Technology, Vol. 204, pp. 1755-1763.

19. **Q. Chang, D.L. Chen, H.Q. Ru, X.Y. Yue, L. Yu and C.P. Zhang**. *Toughening mechanisms in iron-containing hydroxyapatite/titanium composites.* (2010), Biomaterials, Vol. 31, pp. 1493-1501.

20. **W. Que, K.A. Khor, J.L. Xu and L.G. Yu.** *Hydroxyapatite/titania nanocomposites derived by combining high-energy ball milling with spark plasma sintering processes.* (2008), Journal of the European Ceramic Society, Vol. 28, pp. 3083-3090.

21. **X. Zhou and P. Mohanty.** *Electrochemical behavior of cold sprayed hydroxyapatite/titanium composite in Hanks' solution.* (2012), Electrochimica Acta, Vol. 65, pp. 134– 140.

22. **X. Zheng, , M. Huang and C. Ding.** *Bond strength of plasma-sprayed hydroxyapatite/Ti composite coatings.* (2000), Biomaterials, Vol. 21, pp. 841-849.

23. **C. Chu, X. Xue, J. Zhu and Z. Yin.** *In vivo study on biocompatibility and bonding strength of Ti/Ti–20 vol.% HA/Ti–40 vol.% HA functionally graded biomaterial with bone tissues in the rabbit.* (2006), Materials Science and Engineering: A, Vol. 429, pp. 18-24.

24. **T. Kokubo and H. Takadama.** *How useful is SBF in predicting in vivo bone bioactivity?* (2006), Biomaterials, Vol. 27, pp. 2907–2915.

25. **Suryanarayana, C.** *Mechanical alloying and milling.* (2001), Progress in Materials Science, Vol. 46, pp. 1-184.

26. **D. J. Green, O. Guillion, J Rodel.** *Constrained sintering: A delicate balance of scales.* (2008), Journal of the European Ceramic Society, Vol. 28, pp. 1451–1466.